

# Electrocatalytic Oxidation of Methanol on Nickel Doped Metal-Organic Frameworks MIL-110 Modified Glassy Carbon Electrode in Alkaline Medium

Yan Wang<sup>1,†,\*</sup>, Chenglian Liu<sup>1,†</sup>, Jiangnan Xiang<sup>1</sup>, Lei Xing<sup>2</sup>, Xiaoyu Ou<sup>1</sup>, Shili Chen<sup>1</sup>, Xiaojun Xue<sup>1</sup>, Feng Yu<sup>1</sup>, Ruifeng Li<sup>1</sup>

<sup>1</sup>College of Chemistry and chemical Engineering, Taiyuan University of Technology, Shanxi, 030024, China

<sup>2</sup>Institute of Green Chemistry and Chemical Technology, Jiangsu University, Zhenjiang, 212013, China

† These authors contribute equally to this paper.

\*E-mail: [wangyan@tyut.edu.cn](mailto:wangyan@tyut.edu.cn)

Received: 5 January 2019 / Accepted: 20 February 2019 / Published: 10 May 2019

---

Nickel doped metal-organic frameworks MIL-110 catalysts were prepared by impregnation method. The as-prepared Ni/MIL-110 catalysts with different Ni content (10 wt.%, 20 wt.% and 30 wt.%) were characterized by XRD, SEM, elemental distribution analysis, N<sub>2</sub> adsorption-desorption and TEM. Ni/MIL-110 modified glassy carbon electrodes were employed to investigate the methanol electrooxidation reaction (MOR) in 0.1 M NaOH by cyclic voltammetry (CV) and chronoamperometry (CA). Ni/MIL-110 shows good electrocatalytic activity toward MOR and MOR reaction is under diffusion controlled. And the catalytic rate constant is calculated to be  $0.96 \times 10^3 \text{ cm}^3 \text{ mol}^{-1} \text{ s}^{-1}$  by CA analysis.

---

**Keywords:** Alkaline medium, Glassy Carbon Electrode, Metal-organic Frameworks, Methanol Electrooxidation

## 1. INTRODUCTION

Energy crisis is a common problem faced by all countries in the world nowadays. Researchers are trying to develop renewable energy sources or high efficient means of energy utilization to ease the energy crisis. Fuel cells are the promising candidates for efficient energy storage and conversion. Among various types of fuel cells, direct methanol fuel cells (DMFCs) have attracted enormous attention due to their high power density, low-cost, low operating temperature and low pollution [1, 2]. Several technical obstacles need to be overcome before the commercialization of DMFCs. One

example is the sluggish kinetics of the methanol oxidation reaction (MOR) on anode in comparison with the oxygen reduction reaction (ORR) on the cathode in acid medium [3]. The kinetics of MOR with respect to Pt-based alloys have been extensively studied. It was found that the rate limiting elementary step is the dehydrogenation of CH<sub>3</sub>OH absorbed on the Pt sites in acidic environment [4-6]. In contrast, the electrocatalytic oxidation of methanol is kinetically faster in alkaline medium [7]. Therefore, the compatibility of ORR on cathode and MOR on anode could be improved. Moreover, operating DMFCs in alkaline electrolytes offers other advantages such as low corrosiveness and less sensitive to poisons [8, 9]. However, the most commonly used costly Pt-based catalysts are suffering from CO poisoning and the kinetics of methanol electrooxidation on Pt-based catalysts are still slow. Therefore, it is imperative to develop low cost MOR catalyst with improved kinetics and low oxidation overpotential.

In alkaline medium, many low cost non-noble transition metals such as Ni can be a promising candidate as MOR catalysts on anode to replace the traditional used high cost Pt-based catalysts [10]. For preparation of electrocatalysts, porous materials such as zeolites [11], metal-organic frameworks (MOFs)[12, 13] or zeoliticimidazolate frameworks (ZIFs)[14, 15] have been used as the supports due to their large surface area and pore structure which benefit the dispersion of metal species and facilitate the diffusion of electroactive species. Various kinds of nickel supported porous material have been investigated as MOR catalysts and exhibit good electrocatalytic performance in alkaline electrolytes [15-17]. Recently, MOFs-derived materials have been widely investigated for electrochemical energy conversion and storage due to their unique textural and physicochemical properties.

In this paper, porous Al-benzenetricarboxylates MIL-110 (MIL-110(Al)) were synthesized and then nickel species were impregnated in the structure of MIL-110(Al) to fabricate Ni doped MIL-110 catalysts (Ni/MIL-110) for methanol electrooxidation reaction. The electrocatalytic activity of Ni/MIL-110 was investigated by cyclic voltammetry (CV) and chronoamperometry in alkaline electrolytes.

## 2. EXPERIMENTAL

### 2.1 Preparation of Ni/MIL-110

Porous Al-benzenetricarboxylates (Al-BTCs) MIL-110 were synthesized from trimethyl 1,3,5-benzenetricarboxylate (Me<sub>3</sub>-BTC, 98%), aluminum nitrate nonahydrate (Al(NO<sub>3</sub>)<sub>3</sub>·9H<sub>2</sub>O), sodium hydroxide (NaOH, 4 M), nitric acid (HNO<sub>3</sub>, 4 M) and deionized water described in the literature [18]. The reactant compositions were as follows: 1.0 Al(NO<sub>3</sub>)<sub>3</sub>·9H<sub>2</sub>O: 0.5 Me<sub>3</sub>-BTC: 2.3 NaOH: 310 H<sub>2</sub>O. All reactants all mixed thoroughly and then the pH was adjusted to 3.9 by using nitric acid. The mixtures were transferred into Teflon autoclave, which was sealed and heated at 210°C for 3 h. After crystallization, the autoclave was cooled down to room temperature and the solid products were washed by deionized water to pH=7. Then the solid products were washed with N, N-dimethylformamide (DMF) for 5 h to remove the unreacted Me<sub>3</sub>-BTC. Finally, the solid products MIL-110 were recovered by filtration. Ni/MIL-110 catalysts were prepared by impregnation method. Typically, certain amounts of MIL-110 samples and Ni(NO<sub>3</sub>)<sub>2</sub>·6H<sub>2</sub>O was added in DMF solution and

stirred for 3 h. Then Ni/MIL-110 catalysts were obtained after filtration and dried at 100 °C for 12 h. Ni/MIL-110 with different Ni content were denoted as  $x$ Ni/MIL-110, where  $x$  indicates the weight ratio of Ni/MIL-110. 10%Ni/MIL-110, 20%Ni/MIL-110 and 30%Ni/MIL-110 were prepared for further investigation.

## 2.2 Instrumental measurements

X-ray powder diffraction (XRD) patterns were measured on a SHIMADZU XRD-6000 diffractometer using Cu  $K\alpha$  radiation. The morphology and elemental analysis of Ni/MIL-110 were measured by a HITACHI S-4800 scanning electron microscope (SEM) equipped with an energy dispersive X-ray (EDX) analyzer.  $N_2$  adsorption-desorption isotherms were measured on Quantachrome NOVA 1200 instrument at 77 K, and Brumauer-Emmett-Teller (BET) surface areas, pore volume and pore size distribution of the samples were determined by analyzing  $N_2$  adsorption-desorption isotherms.

## 2.3 Electrochemical measurements

Cyclic voltammetry (CV) and chronoamperometry (CA) were carried out by using a CHI-600B electrochemical workstation. All electrochemical tests were conducted by using a three-electrode setup with Ag/AgCl (3M KCl) as the reference electrode, Pt wires as the counter electrode and Ni/MIL-110 modified glassy carbon electrode (GCE, geometric area is 0.0707 cm<sup>2</sup>) as working electrode. Catalysts inks were prepared by dispersing 1mg Ni/MIL-110 and 2 mg carbon black ultrasonically in 0.2 mL isopropanol and 0.8 mL 0.05 wt.% Nafion solution. Then, 5 $\mu$ L catalysts ink was pipette directly on the polished surface of GCE and dried in air to obtain Ni/MIL-110 modified GCE.

## 3. RESULTS AND DISCUSSION

### 3.1 Characterization of Ni/MIL-110

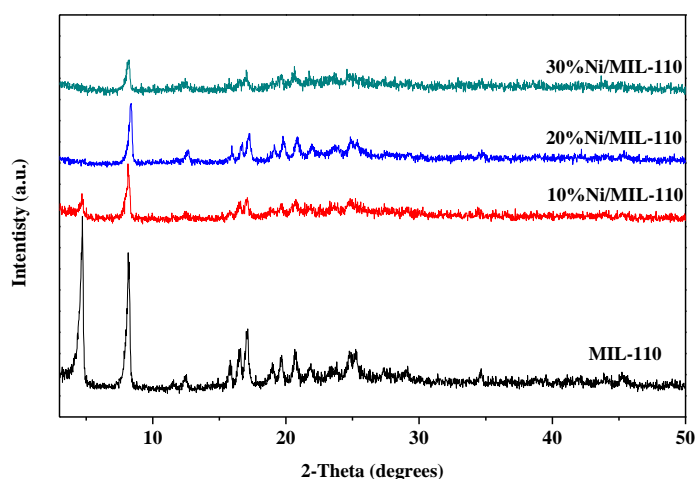


**Figure 1.** XRD patterns of MIL-110(Al) and Ni/MIL-110 with different Ni contents.

XRD patterns of MIL-110 and Ni doped MIL-110 are shown in Figure 1. Strong characteristic diffraction peaks of the as-synthesized MIL-110(Al) could be observed which indicates MIL-110(Al) has been synthesized successfully [18]. After impregnation procedure, the intensity of diffraction peaks decreases dramatically along with Ni content increasing. The diffraction peak at  $4.7^\circ$  decrease especially obvious and this peak even disappear when Ni content is more than 20%. Moreover, no diffraction peaks of nickel species are observed in all samples, which indicates Ni are highly dispersed in Ni/MIL-110 catalysts.

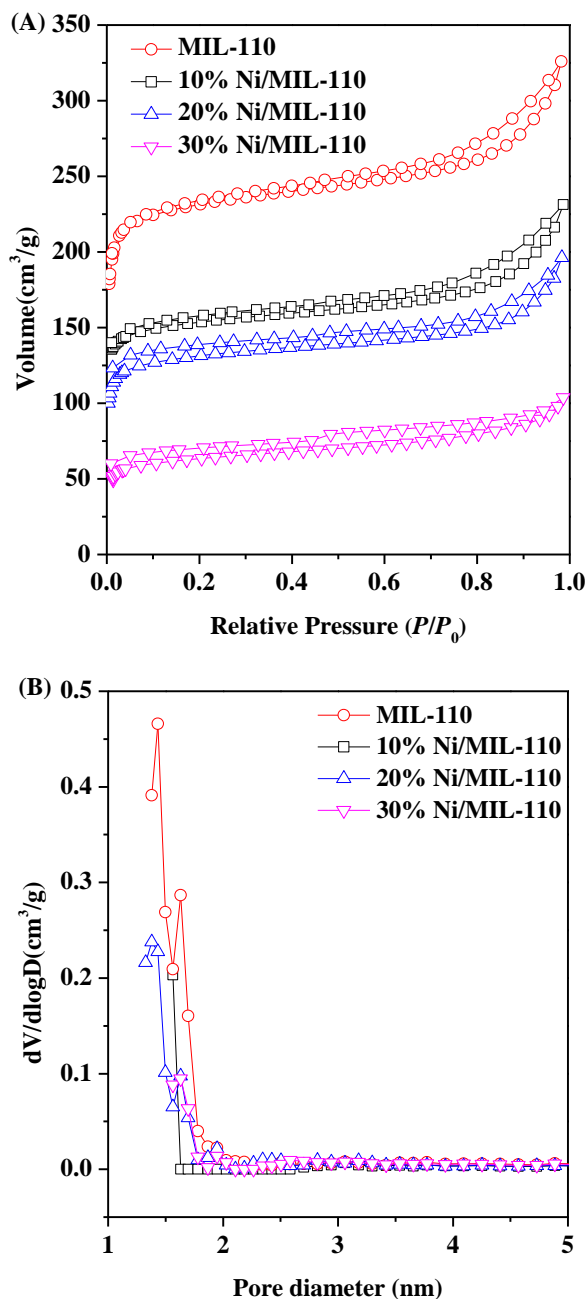
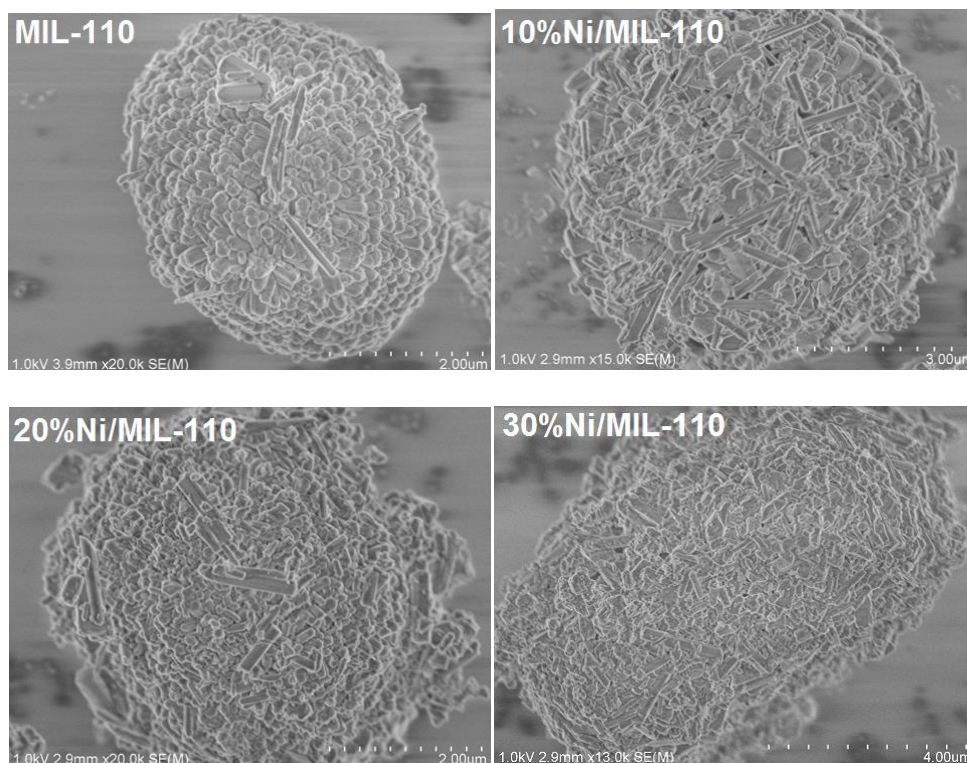


**Figure 2.**  $N_2$  adsorption-desorption isotherms (A) and the corresponding pore size distribution curves (B) of MIL-110 and Ni/MIL-110 with different Ni contents.

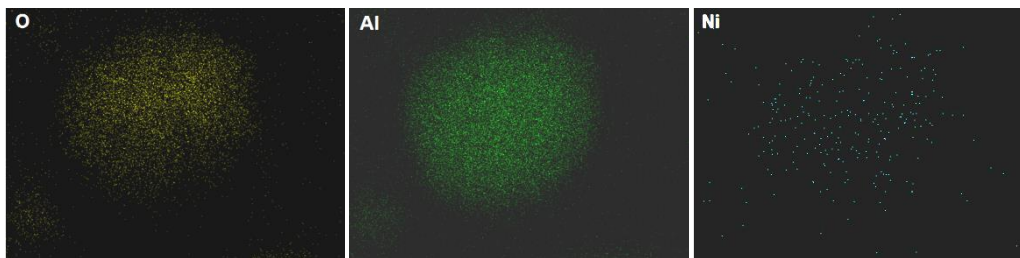
**Table 1.** The structural parameters of samples obtained from N<sub>2</sub> adsorption isotherm analysis.

Samples	S <sub>BET</sub> (m <sup>2</sup> /g)	S <sub>mic</sub> (m <sup>2</sup> /g)	Pore volume (cm <sup>3</sup> /g)		Pore diameter (nm)
			V <sub>mic</sub>	V <sub>meso</sub>	
MIL-110	927	817	0.31	0.18	1.6
10%Ni/MIL-110	608	535	0.21	0.14	1.4
20%Ni/MIL-110	518	447	0.17	0.12	1.6
30%Ni/MIL-110	243	188	0.07	0.08	1.3

N<sub>2</sub> adsorption-desorption isotherms of MIL-100 and Ni/MIL-110 are presented in Figure 2A. All samples show typical type I isotherm at low relative pressure ( $P/P_0 < 0.1$ ), suggesting all these samples obtain microporous structures. From pore size distribution calculated by DFT model, it can be seen that the micropore diameters of all samples are centered at ~1.5 nm. Furthermore, the structural parameters of all samples are summarized in Table 1. The support MIL-110 shows high BET surface area (927 m<sup>2</sup>/g). With the Ni doping content increasing, the BET surface area (S<sub>BET</sub>) and pore volume decrease significantly to 243 m<sup>2</sup>/g and 0.15 cm<sup>3</sup>/g, respectively.



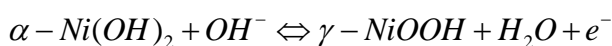
**Figure 3.** SEM images of MIL-110 and Ni/MIL-110 with different Ni contents.



**Figure 4.** EDS mapping analysis of 20%Ni/MIL-110.

The morphology of all samples are investigated by SEM and shown in Figure 3 MIL-110 exhibits sphere assembled by hexagonal prisms morphology. The hexagonal prisms morphology is largely preserved on 10%Ni/MIL-110. However, with the Ni content increasing, the structure of MIL-110 is partially collapsed and the hexagonal prisms morphology can hardly be observed. This result is in consistent with XRD and N<sub>2</sub> adsorption-desorption results. High Ni doping content could jeopardize the structure and crystallinity of MIL-110 supports. Elemental mapping analysis of 20%Ni/MIL-110 is exhibited in Figure4. The result further confirms Ni species are highly dispersed in MIL-110 support.

CVs of Ni doped MIL-110 and MIL-110 in 0.1 M NaOH with 0.1 M methanol at scan rate 10 mV/s are shown in Figure 5. CV of 20%Ni/MIL-110 in absence of methanol in 0.1 M NaOH electrolytes is also shown in Figure 6. In alkaline electrolyte, a layer of Ni(OH)<sub>2</sub> can be formed spontaneously on the surface of Ni based catalysts [19]. According to literature report, two peaks at low potential (~0.53 V) and at high potential (~0.74 V) on CVs of Ni based catalysts can be observed which can be allocated to  $\alpha$ -Ni(OH)<sub>2</sub>/NiOOH conversion  $\beta$ -Ni(OH)<sub>2</sub>/NiOOH conversion, respectively [20]. However, only one peak in the anodic direction at 0.55 V can be observed on CV of 20%Ni/MIL-110 in absence of methanol, and no significant oxidation peak of  $\beta$ -Ni(OH)<sub>2</sub> can be observed on 20%Ni/MIL-110 in 0.1 M NaOH electrolyte. The peak at 0.55 V can be attributed to the oxidation of  $\alpha$ -Ni(OH)<sub>2</sub> to nickel oxy-hydroxide (NiOOH) according the following reaction [21]:



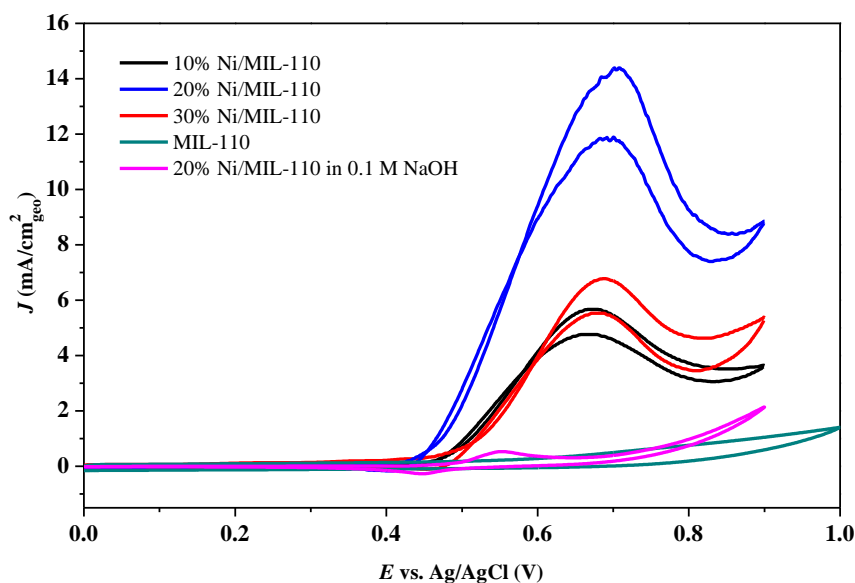
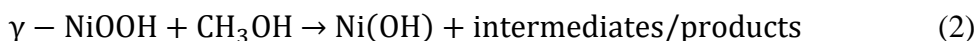


**Figure 5.** CVs of 10%Ni/MIL-110, 20%Ni/MIL-110, 30%Ni/MIL-110 andMIL-110 in 0.1 M NaOH with 0.1 M methanol at scan rate 10 mV/s.

In alkaline electrolyte,  $\alpha$ -Ni(OH)<sub>2</sub> and  $\beta$ -Ni(OH)<sub>2</sub> are oxidized to  $\gamma$ -NiOOH and  $\beta$ -NiOOH, respectively [21]. Compared with  $\beta$ -Ni(OH)<sub>2</sub>,  $\alpha$ -Ni(OH)<sub>2</sub> is unstable and easily convert into  $\beta$ -Ni(OH)<sub>2</sub> in alkaline media. However,  $\alpha$ -Ni(OH)<sub>2</sub> can be stabilized by introducing Al in the Ni(OH)<sub>2</sub> lattice [21]. Thus, the MIL-110 supports stabilize  $\alpha$ -Ni(OH)<sub>2</sub>, causing the formation of  $\gamma$ -NiOOH in Ni/MIL-110 catalysts. Meanwhile, a peak in the cathodic direction at 0.44 V can be attributed to the reduction of NaOOH to Ni(OH)<sub>2</sub>[22]. At potentials higher than 0.8 V, oxygen evolution reaction (OER) occurs in all catalysts which originates from OH<sup>-</sup>oxidation. In comparison CV of MIL-110 in 0.1 M methanol in 0.1 M NaOH, considerable anodic currents are observed on all Ni/MIL-110 catalysts which attribute to the methanol electrooxidation. There is no obvious peak of methanol electrooxidation on CV of MIL-110 could be observed. This result suggests NiOOH species work as the active sites for methanol electrooxidation. At the reverse scan, there are oxidation peaks at ~0.68 V on CVs of Ni/MIL-110 which indicate the regeneration of active sites for methanol adsorption at higher potential value. The reduction peaks at 0.44 V on CVs of Ni/MIL-110. However, the current values are much lower than that on 20%Ni/MIL-110 in 0.1 M NaOH. The decrease of reduction current value is attributed to partial consumption of  $\gamma$ -NiOOH for methanol electrooxidation. From the above experimental result, a plausible mechanism of methanol electrooxidation could be proposed as follows:



In this equation, the products of methanol electrooxidation include the intermediates/products such as formaldehyde, carbonate and formate ions[10].

Table 2 presents the peak current density and the peak potential for methanol electrooxidation on various Ni doped catalysts in previously reported literatures. In comparison with other Ni doped porous materials (zeolites or  $\text{Al}_2\text{O}_3$ ), Ni doped MOFs (Ni/MIL-110) shows the highest current density and the lowest peak potential which suggests Ni/MIL-110 could be a competitive candidate for methanol electrooxidation in alkaline electrolytes. Among Ni/MIL-110 with different Ni contents, 20%Ni/MIL-110 exhibits the highest current density for methanol electrooxidation. 10%Ni/MIL-110 shows the lowest activity due to its relatively low Ni content. However, 30%Ni/MIL-110 exhibits much lower activity toward methanol electrooxidation compared with 20%Ni/MIL-110 due to the fact that its structure and Ni dispersion have been largely sacrificed during nickel doping procedure.

**Table 2.** Comparison of the peak current density ( $J$ ) and the peak potential ( $E_p$ ) reported in literatures for methanol electrooxidation on various Ni based electrodes.

Electrodes	$J$ ( $\text{mA}/\text{cm}^2$ )	$E_p$ (V vs. Ag/AgCl)	$\nu$ ( $\text{mV}/\text{s}$ )	References
Ni-P/CPE <sup>a</sup>	13.75	0.80	25	[23]
Ni-ZSM-5/CPE	9.2	0.72	20	[24]
Ni-Y/CPE	5.5	0.78	20	[25]
Ni-SBA-15/CPE	14.2	0.81	25	[16]
Ni-SBA-16/CPE	16.63	0.76	25	[26]
Ni- $\text{Al}_2\text{O}_3$ /GCE	11.1	0.72	20	[17]
10%Ni/MIL-110	5.7	0.67	10	this work
20%Ni/MIL-110	14.4	0.70	10	this work
30%Ni/MIL-110	6.9	0.69	10	this work

<sup>a</sup> CPE, Carbon Paste Electrode.

CVs of 20%Ni/MIL-110 in 0.1 M NaOH with 0.1 M methanol at different scan rates are shown in Figure 6A. With the scan rates increasing, the anodic peak potentials shift to positive potentials and the cathodic peak potentials shift to negative potential, which indicate a kinetic limitation k methanol electrooxidation. Meanwhile, the plot of the anodic peak current ( $I_{pa}$ ) versus the square root of scan rates ( $\nu^{1/2}$ ) shows a linear dependence in scan rates of 1-150 mV/s (Figure 6B), suggesting the methanol electrooxidation process is under a diffusion control rather than a surface control. A linear dependence is also observed between in the plot of  $\log I_{pa}$  versus  $\log \nu$  (Figure 6C), and the slope is calculated to be 0.352. In theory, a slope of  $\log I_{pa}$  versus  $\log \nu$  is 1.0 or 0.5, which is regarded as methanol electrooxidation is under adsorption or diffusion controlled, respectively [16]. The slope of

0.352 is obtained that is near the theoretically value of 0.5 for a diffusion controlled process. This relatively low value indicates the charge transfer on Ni/MIL-110 is slow and methanol electrooxidation is controlled by combined kinetic and diffusion limitation.

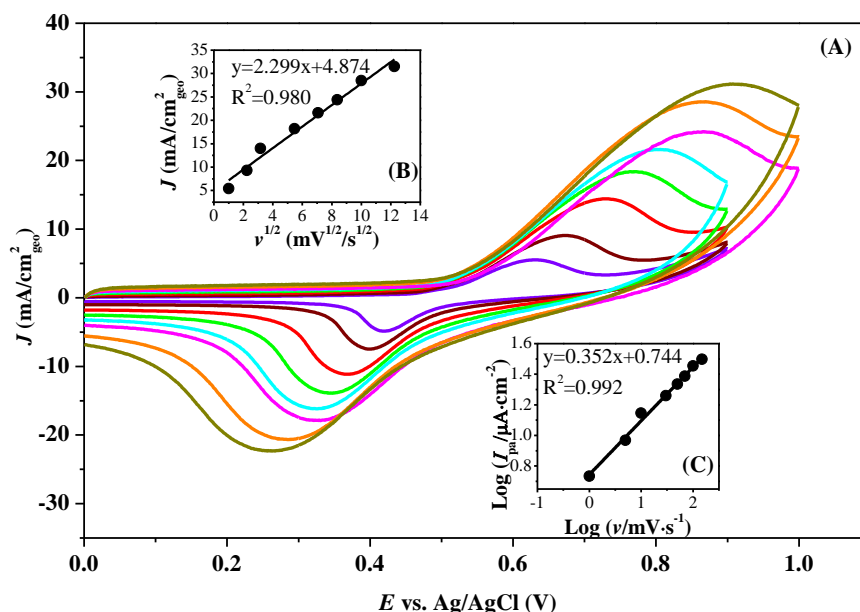


**Figure 6.** (A) CVs of 20% Ni/MIL-110 in 0.1 M NaOH with 0.1 M methanol at different scan rates (from inner to outer): 1, 5, 10, 30, 50, 70, 100, 150 mV/s. (B) A plot of the anodic peak current density ( $I_{pa}$ ) versus the square root of scan rates ( $v^{1/2}$ ). (C) A plot of  $\log I_{pa}$  versus  $\log v$ .

The diffusion coefficient of methanol and the catalytic rate constant on Ni/MIL-110 modified GCE have been measured by chronoamperometry method. Figure 7A shows the double-step chronoamperograms by setting the potential of Ni/MIL-110 modified GCE at 700 mV (in first step) and 300 mV (in second step) determined by the peak potential of redox process at various concentrations of methanol. The plots of  $I_{net}$  (the net current density, obtained by subtracting the background current) vs.  $t^{-1/2}$  (Figure 7B) shows a linear dependence, which suggests a methanol diffusion controlled behavior. The value of diffusion coefficient ( $D$ ) is calculated to be  $2.08 \times 10^{-3} \text{ cm}^2/\text{s}$  by using the slope of  $I_{net}$  vs.  $t^{-1/2}$  modeled by Cottrell equation[27]:

$$I_{net} = nFAD^{1/2}c\pi^{1/2}t^{-1/2}$$

$$I_{net} = nFAD^{1/2}c\pi^{-1/2}t^{-1/2} \tag{3}$$

where  $F$  is the Faraday’s constant,  $A$  is electrode area ( $\text{cm}^2$ ),  $c$  is the concentration of methanol (mol/L),  $n$  is the total number of electron transfer,  $D$  is the diffusion coefficient. In alkaline medium, methanol oxidation is regarded through a four electron process on Ni based catalysts[28]. Moreover, the catalytic rate constant ( $k_{cat}$ ) of methanol oxidation is calculated from the following equation[27]:

$$I_{net}/I_L = \pi^{1/2}(k_{cat}ct)^{1/2}$$

$$I_{cat}/I_L = \pi^{1/2}(k_{cat}ct)^{1/2} \quad (4)$$

where  $I_{cat}$  and  $I_L$  are the current density in presence and absence of methanol, respectively. And  $k_{cat}$ ,  $c$  and  $t$  represent the catalytic rate constant ( $\text{cm}^3 \text{mol}^{-1} \text{s}^{-1}$ ), methanol concentration (mol/L) and time (s), respectively. The value of  $k_{cat}$  is  $0.96 \times 10^3 \text{cm}^3 \text{mol}^{-1} \text{s}^{-1}$  calculated from the slope of  $I_{cat}/I_L$  vs.  $t^{1/2}$  (Figure 7C). This result confirms that Ni/MIL-110 shows a good methanol electrooxidation activity.

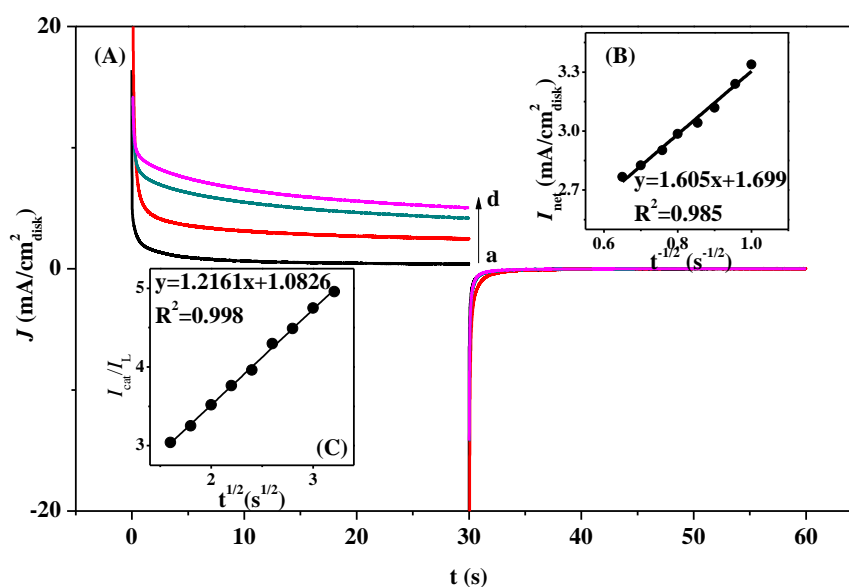


**Figure 7.** (A) Chronoamperograms of 20% Ni/MIL-110 in 0.1 M NaOH solution containing (a) 0 M, (b) 0.05 M, (c) 0.1 M, (d) 0.2 M methanol. Inset (B): Plots of net current  $I_{net}$  vs.  $t^{-1/2}$ , derived from the data of chronoamperograms. Inset (C): Plots of  $I_{cat}/I_L$  vs.  $t^{1/2}$ , derived from the data of chronoamperograms.

#### 4. CONCLUSIONS

Nickel doped MIL-110 catalysts have been prepared by impregnation method and have been employed as the catalysts for methanol electrooxidation reaction (MOR). Ni/MIL-110 catalyst obtains high surface area and high nickel dispersion. With nickel content increasing, the structure of MIL-110 has been partly destroyed due to high nickel doping content. Methanol electrooxidation behaviors have been investigated by CVs and chronoamperometry methods. The results indicate a good activity toward methanol electrooxidation in alkaline electrolytes and methanol oxidation is mainly under

methanol diffusion control. Moreover, the catalytic rate constant of methanol electrooxidation is obtained to be  $0.96 \times 10^3 \text{ cm}^3 \text{ mol}^{-1} \text{ s}^{-1}$  by chronoamperometric analysis.

#### ACKNOWLEDGEMENTS

This work is supported by the Natural Science Foundation for Young Scientists of Shanxi Province, China (Grant No.201701D221040), Shanxi Provincial Key Innovative Research Team in Science and Technology (No.2014131006), Natural Science Foundation of Jiangsu Province of China (BK20170530), Startup funding for young researchers of Jiangsu University of China (16JDG061), and the joint funds of the National Natural Science Foundation of China–China Petroleum and Chemical Corporation (the state key program grant No.U1463209).

#### References

1. C. Bianchini and P.K. Shen, *Chem. Rev.*, 109 (2009) 4183.
2. K. Scott and L. Xing, *Advances in Chemical Engineering*, (2012) Elsevier, Holland.
3. J. Wang, J. Xi, Y. Bai, Y. Shen, J. Sun, L. Chen, W. Zhu and X. Qiu, *J. Power Sources*, 164 (2007) 555.
4. Y.-P. Sun, L. Xing, K. Scott, *J. Power Sources*, 195 (2010) 1.
5. L. Xing, K. Scott and Y.-P. Sun, *Int. J. Electrochemistry*, (2011)853261.
6. Q. Xu, W. Zhang, J. Zhao, L. Xing, Q. Ma, L. Xu and H. Su, *Int. J. Green Energy*, 15 (2018) 181.
7. J.-H. Kim, H.-K. Kim, K.-T. Hwang and J.-Y. Lee, *Int. J. Hydrogen Energy*, 35 (2010) 768.
8. E.R. Choban, J.S. Spendelow, L. Gancs, A. Wieckowski and P.J.A. Kenis, *Electrochim. Acta*, 50 (2005) 5390.
9. E.H. Yu and K. Scott, *J. Appl. Electrochem.*, 35 (2005) 91.
10. J.-B. Raoof, R. Ojani and S.R. Hosseini, *J. Power Sources*, 196 (2011) 1855.
11. B. Kaur, R. Srivastava and B. Satpati, *ACS Catalysis*, 6 (2016) 2654.
12. A. Akinpelu, B. Merzougui, S. Bukola, A.-M. Azad, R.A. Basheer, G.M. Swain, Q. Chang and M. Shao, *Electrochim. Acta*, 161 (2015) 305.
13. E.M. Miner, S. Gul, N.D. Ricke, E. Pastor, J. Yano, V.K. Yachandra, T. Van Voorhis and M. Dincă, *ACS Catalysis*, 7 (2017) 7726.
14. J. Li, Q.-L. Zhu and Q. Xu, *Chem. Commun.*, 51 (2015) 10827.
15. A. Samadi-Maybodi, S. Ghasemi and H. Ghaffari-Rad, *J. Power Sources*, 303 (2016) 379.
16. S.N. Azizi, S. Ghasemi and E. Chiani, *Electrochim. Acta*, 88 (2013) 463.
17. Y. Wang, D. Pan, Q. Xu, J. Ma, J. Zheng and R. Li, *Int. J. Electrochem. Sci.*, 12 (2017) 2194.
18. N.A. Khan, J.S. Lee, J. Jeon, C.-H. Jun and S.H. Jung, *Microporous and Mesoporous Mat.*, 152 (2012) 235.
19. F. Hahn, D. Floner, B. Beden and C. Lamy, *Electrochim. Acta*, 32 (1987) 1631.
20. Q. Yi, J. Zhang, W. Huang and X. Liu, *Catal. Commun.*, 8 (2007) 1017.
21. Z. Mojović, P. Banković, N. Jović-Jovičić A. Milutinović-Nikolić, A. Abu Rabi-Stanković and D. Jovanović, *Int. J. Hydrogen Energy*, 36 (2011) 13343.
22. Y.-C. Weng, J.F. Rick and T.-C. Chou, *Biosens. Bioelectron.*, 20 (2004) 41.
23. S.N. Azizi, S. Ghasemi and F. Amiripour, *Electrochimica Acta*, 137 (2014) 395.
24. J.B. Raoof, N. Azizi, R. Ojani, S. Ghodrati, M. Abrishamkar and F. Chekin, *Int. J. Hydrogen Energy*, 36 (2011) 13295.
25. R. Ojani, J.-B. Raoof, S. Fathi and S. Alami-Valikchali, *J. Solid State Electrochem.*, 15 (2011) 1935.
26. S.N. Azizi, S. Ghasemi and H. Yazdani-Sheldarrei, *Int. J. Hydrogen Energy*, 38 (2013) 12774.
27. I. Danaee, M. Jafarian, F. Forouzandeh, F. Gobal and M.G. Mahjani, *Int. J. Hydrogen Energy*, 33

(2008) 4367.

28. A.N. Golikand, S. Shahrokhian, M. Asgari, M. Ghannadi Maragheh, L. Irannejad and A. Khanchi, *J. Power Sources*, 144 (2005) 21.

© 2019 The Authors. Published by ESG ([www.electrochemsci.org](http://www.electrochemsci.org)). This article is an open access article distributed under the terms and conditions of the Creative Commons Attribution license (<http://creativecommons.org/licenses/by/4.0/>).